# RING SMRA 16-17285-01 - CU ALLOY - ROMAN TIMES - SWITZERLAND

**Artefact name** Ring SMRA 16-17285-01

**Authors** Christian. Degrigny (HE-Arc CR, Neuchâtel, Neuchâtel, Switzerland) & Naima. Gutknecht (HE-Arc CR, Neuchâtel, Neuchâtel, Switzerland) & Valentina. Valbi (Laboratoire Métallurgie et Culture LMC-IRAMAT-CNRS-UTBM, Belfort, Franche-Comté, France)

**Url** /artefacts/1324/

## The object

*Credit SMRA*

Fig. 1: Ring (face A and side views),

## Description and visual observation

**Description of the artefact** Ring with a faceted cross-section and decorated with ridges on the outside. Its original shape seems to be preserved although the brown corrosion structure is heavily cracked and even has a large lacuna on face A (Fig. 1). Diameter (external) = 2.6cm and weight = 2.5g.

**Type of artefact** Jewellery

**Origin** Avenches, Switzerland, Avenches, Vaud, Switzerland

**Recovering date** 2016

**Chronology category** Roman Times

**chronology tpq** ----

**chronology taq** ----

**Chronology comment**

**Burial conditions / environment** Soil

**Artefact location** Site et musée romains Avenches, Avenches, Vaud

**Owner** Site et musée romains Avenches, Avenches, Vaud

**Inv. number** SMRA 16/17285-01

**Recorded conservation data** Cleaning of soil with ethanol and consolidation with resin paraloid B72 in ethyl acetate. Drying at 50°C.

## Complementary information

The object was found at Milavy, a village near Avenches.
Flaking of the surface was observed before the drying of the object, hence the consolidation with paraloid B72.

## Study area(s)


*Credit SMRA / HE-Arc CR, N.Gutknecht.*

Fig. 2: Location of XRF analyses (red circles), Fig. 3 (blue square) and Fig. 6 (Raman spectroscopy (blue square)) on face A,

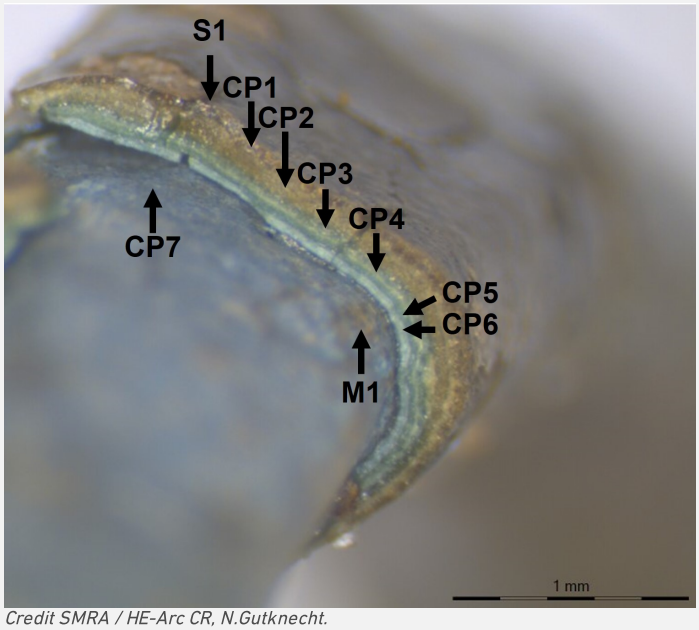


*Credit SMRA / HE-Arc CR, N.Gutknecht.*

Fig. 3: Description of the corrosion structure,

## Binocular observation and representation of the corrosion structure

The schematic representation below gives an overview of the corrosion structure encountered on the ring from a first visual macroscopic observation.
There are cracks through CP1 to CP6 that generate the flaking of the layers.

| Stratum | Type of strata | Principal characteristics |
|---|---|---|
| S1 | Soil | light brown, thin, scattered, matte |
| CP1 | Corrosion product | brown, thin, discontinuous, matte, network of cracks |
| CP2 | Corrosion product | light brown, thick, discontinuous, matte, network of cracks |
| CP3 | Corrosion product | light green, thin, discontinuous, matte, compact, friable, soft, network of cracks |
| CP4 | Corrosion product | pale turquoise, thin, discontinuous, matte, compact, friable, soft, network of cracks |
| CP5 | Corrosion product | light green, medium, discontinuous, matte, compact, friable, soft, network of cracks |
| CP6 | Corrosion product | pale turquoise, medium, discontinuous, matte, compact, friable, soft, network of cracks |
| CP7 | Corrosion product | blue, thin, discontinuous, matte, non compact, friable, soft, no crack, microstructure of black spots |
| M1 | Metal | yellow, thick, continuous, metallic, compact, tough, soft, no crack |

Table 1: Description of the principal characteristics of the strata as observed under binocular and described according to Bertholon's method.

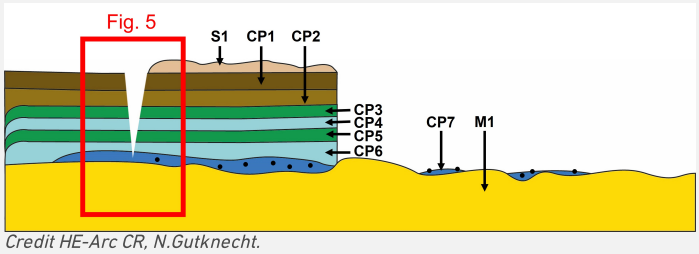


*Credit HE-Arc CR, N.Gutknecht.*

Fig. 4: Stratigraphic representation of the corrosion structure of the ring by macroscopic and binocular observation with indication of the corrosion structure used to build the MiCorr stratigraphy of Fig. 5 (red rectangular),

## MiCorr stratigraphy(ies) – Bi

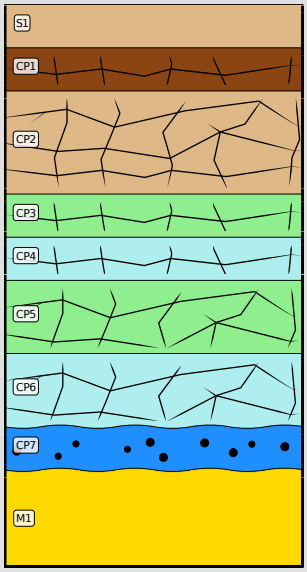


Fig. 5: Stratigraphic representation of the corrosion structure of the ring observed macroscopically under binocular using the MiCorr application with reference to Fig. 4. The characteristics of the strata, such a discontinuity, are accessible by clicking on the drawing that redirects you to the search tool by stratigraphy representation, Credit HE-Arc CR, N.Gutknecht.

## Sample(s)

| | |
|---|---|
| **Description of sample** | No sample was taken. The examination was carrried out directly on the object. |
| **Alloy** | Cu Alloy |
| **Technology** | Unknown |
| **Lab number of sample** | None |
| **Sample location** | None |
| **Responsible institution** | None |
| **Date and aim of sampling** | |

### Complementary information

The ring was probably made by casting and cold-working.

## Analyses and results

*Analyses performed:*

**Non-invasive approach**

- XRF with handheld portable X-ray fluorescence spectrometer (NITON XL3t 950 Air GOLDD+, Thermo Fischer®). General Metal mode, acquisition time 60s (filters: Li20/Lo20/M20).
- Optical microscopy: the object is observed using a numerical microscope KEYENCE VHX-7000 in dark field.

- µ-Raman spectroscopy: it is performed on a HORIBA Labram Xplora spectrometer equipped with a 532 nm laser with 1800 grating, the laser power employed is between 0.04 and 0.55 mW with acquisition time varying between 1 and 5 minutes.

## Non invasive analysis

XRF analysis was carried out without sampling. For point 1, all strata (soil, corrosion products, and metal) are analyzed at the same time. As for point 2, the analysis was performed where corrosion layers flaked. Therefore, it reflects better the metal composition. The metal is presumably a copper-tin alloy with some lead, while the Si, Fe, Al and P are probably coming from the burial environment. The higher amount of tin on point 1 (with corrosion layers) than on point 2 (corrosion structure flaked, metal visible) is a strong indicator of tin enrichment on the corrosion layers. The presence of chlorine could not be revealed.

| Elements (mass%) | 1 | σ | 2 | σ |
|---|---|---|---|---|
| Cu | 20.2 | 0.1 | 73.9 | 0.19 |
| Sn | 67.1 | 0.21 | 15.8 | 0.08 |
| Pb | 0.8 | 0.02 | 0.4 | 0.02 |
| P | 2.3 | 0.05 | 2.4 | 0.06 |
| Si | 3.8 | 0.09 | 4.7 | 0.13 |
| Fe | 2.9 | 0.08 | 0.2 | 0.015 |
| Al | 2.1 | 0.17 | 1.2 | 0.19 |
| S | n.d. | n.d. | 0.5 | 0.02 |
| As | 0.2 | 0.02 | 0.3 | 0.02 |

Table 2: Chemical composition analysed with handled XRF at the surface of the ring for two representative points shown in Fig.2. The results are rounded up to the nearest whole number (n.d.: below the detection limit), UR-Arc CR.

It was not possible to sample this artefact. Therefore, µ-Raman point analyses were performed on the surface of the object in an area where different strata of corrosion products were exposed, as shown in Fig. 6 in a micrograph taken by optical microscopy. The surface of the object appears brown (CP1). It covers a green stratum (CP5) and a blue/golden one (CP7 and M1) with black spots in it. The R01 analysis point was performed on one of the black spots observed in the blue stratum and can be identified as covellite (CuS) by comparison with a reference spectrum. Point analyses performed on the blue (CP7) and golden stratum showed a spectrum with a large peak at around 560 cm-1 (R09) that can be identified as nanocassiterite ($SnO_2$) by comparison with the work of Ospitali et al. 2012. The R03 point analysis was performed on the green stratum (CP5) and is identified as malachite ($Cu_2(CO_3)(OH)_2$) by comparison with a reference spectrum.

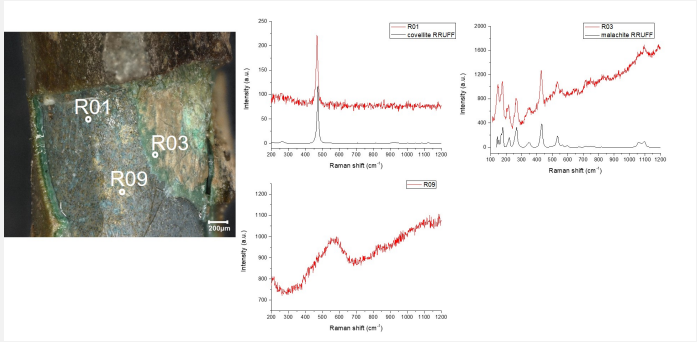


*Credit LMC-CNRS, V.Valbi.*

Fig. 6: Raman points of analysis on the surface of the object and Raman spectra obtained for R01(together with the covellite reference spectrum RRUFFID=R060306), R03 (together with the malachite reference spectrum RRUFFID=R050508) and R09,

## Metal

According to the XRF results (table 2, point 2) the metal is probably a tin bronze alloy with some lead.
The presence of chlorine was not investigated.

| | |
|---|---|
| **Microstructure** | None |
| **First metal element** | Cu |
| **Other metal elements** | Sn, Pb |

**Complementary information**

None.

## Corrosion layers

A tin enrichment is clearly observed in the top corrosion layers of the corrosion structure (see table 2).

| | |
|---|---|
| **Corrosion form** | Uniform |
| **Corrosion type** | Unknown |

**Complementary information**

None.

## MiCorr stratigraphy(ies) – CS

## Synthesis of the binocular / cross-section examination of the corrosion structure

No documentation was done in cross-section since no sample could be taken. Therefore the documentation in binocular view is the only one available.

## Conclusion

The ring is a tin bronze probably with some lead. The identification of nanocassiterite as the most internal CP shows a phenomenon of decuprification typical of bronze corrosion, accompanied by the formation of copper hydroxycarbonate as a more external CP. The dark inclusions observed in the CP7 and identified as covellite are likely to be residuals of copper sulfide inclusions from the metal microstructure.

The limit of the original surface is probably located between CP1 and S1 since there is surface decoration at this level. The flaking is taking away locally the original surface.

This artefact is part of a corpus of objects, together with a roman Fibula SMRA20/19066-1 and Earstick SMRA 20/19047-03, which show flaking corrosion products.

## References


**References on object and sample**

1. MiCorr_Earstick SMRA 20/19047-03
2. MiCorr_Fibula SMRA20/19066-10

**References on analytical methods and interpretation**

3. Lafuente, B., Downs, R. T., Yang, H., Stone, N. (2015) The power of databases: the RRUFF project. In: Highlights in Mineralogical Crystallography, T. Armbruster and R. M. Danisi, eds. Berlin, Germany, W. De Gruyter, 1-30.
4. Ospitali, F., Chiavari, C., Martini, C., Bernardi, E., Passarini, F., Robbiola, L. (2012) The characterization of Sn-based corrosion products in ancient bronzes: a Raman approach. Journal of Raman Spectrpscopy, 43 (11), 1596-1603.
5. Robbiola, L., Blengino, M., Fiaud, C., (1998) Morphology and mechanisms of formation of natural patinas on archaeological Cu–Sn alloys. Corrosion Science, 40 (12), 2083-2111.